



THE UNIVERSITY *of* EDINBURGH

Edinburgh Research Explorer

## Eruption of crystal mush and the formation of steep-sided volcanic domes on Venus

**Citation for published version:**

Bromiley, GD & Law, S 2020, 'Eruption of crystal mush and the formation of steep-sided volcanic domes on Venus: Insight from picritic bodies near Marki, Cyprus', *Icarus*, vol. 337, 113467.  
<https://doi.org/10.1016/j.icarus.2019.113467>

**Digital Object Identifier (DOI):**

[10.1016/j.icarus.2019.113467](https://doi.org/10.1016/j.icarus.2019.113467)

**Link:**

[Link to publication record in Edinburgh Research Explorer](#)

**Document Version:**

Peer reviewed version

**Published In:**

*Icarus*

**General rights**

Copyright for the publications made accessible via the Edinburgh Research Explorer is retained by the author(s) and / or other copyright owners and it is a condition of accessing these publications that users recognise and abide by the legal requirements associated with these rights.

**Take down policy**

The University of Edinburgh has made every reasonable effort to ensure that Edinburgh Research Explorer content complies with UK legislation. If you believe that the public display of this file breaches copyright please contact [openaccess@ed.ac.uk](mailto:openaccess@ed.ac.uk) providing details, and we will remove access to the work immediately and investigate your claim.



1 **Eruption of crystal mush and the formation of steep-sided volcanic domes on**  
2 **Venus: insight from picritic bodies near Marki, Cyprus.**

3  
4 **Geoffrey D. Bromiley\* and Sally Law**

5  
6 *School of GeoSciences, Grant Institute, King's Buildings, University of Edinburgh, EH9 3FE,*  
7 *UK*

8  
9 \*corresponding author: geoffrey.bromiley@ed.ac.uk, +44 (0)131 6508519

10  
11 Key words: Venus; volcanism; crystal mush: steep-sided dome

12  
13  
14  
15 **Highlights:**

- 16
- 17 • Steep volcanic domes on Venus form by enigmatic eruption of viscous lava
  - 18
  - 19 • New model proposes that they represent fault-controlled extrusion of crystal mush
  - 20
  - 21 • Implies common magmatic origin for domes and associated, extensive basaltic terrains
  - 22
  - 23 • Extrusion mechanism could occur on other stagnant-lid planetary bodies
  - 24
  - 25
  - 26

27 Declarations of interest: none

## 32 **Abstract**

33

34 Steep-sided domes are one of the most striking volcanic landforms on Venus. They may  
35 also be key to determining the range of magmatic processes operating on Venus as, in  
36 contrast to all other volcanic landforms, they likely represent eruption of viscous lava.  
37 Although there have been various explanations for the presence of high-viscosity lavas on a  
38 planet dominated by effusive basaltic volcanism, it is often assumed that they are silica-rich.  
39 This would necessitate either periodic, large-scale, extensive fractionation of basaltic magma  
40 in the Venusian crust, or a mechanism for re-melting an already silica-enriched lower crust.  
41 As such, determining the origin of steep-sided domes is important in constraining magmatic  
42 processes on Venus, and for understanding geological evolution of stagnant lid regime  
43 planets generally. Here, we use observations from the Marki region of the Troodos ophiolite,  
44 Cyprus, to propose an alternative model where steep-sided domes form by eruption of  
45 crystal mush from the same magmatic systems which fed extensive basaltic terrains with  
46 which domes are associated. Steep-sided volcanic landforms near Marki represent extrusion  
47 of 'un-eruptible', extremely olivine-rich mush onto the palaeo-seafloor, following cessation of  
48 widespread basaltic volcanism. Field relations suggest that these bodies formed by  
49 localised, repeated extrusion of crystal mush, fed by extensional faults tapping crustal  
50 magma chambers. Differential stress enabled eruption of viscous, non-Newtonian magmas  
51 with crystal contents >50 vol%, which then built up volcanic edifices on the seafloor. A  
52 similar, much larger-scale, mechanism can explain many features of steep-sided volcanic  
53 domes on Venus, including their intimate relationship with extensive, basaltic terrains,  
54 general morphology, and dome spatial and temporal clustering. This implies that domes  
55 share a common magmatic origin with the Venusian basaltic crust, rather than representing  
56 a discrete magmatic process, and that they represent periods of magmatic quiescence. It  
57 also implies that the contrasting morphology of these domes arises from a fundamental  
58 difference in eruptive style, from widespread effusive basaltic magmatism to localised,  
59 extensional fault-controlled extrusion of crystal mush. If correct, this mechanism might also  
60 explain formation of steep-sided volcanic edifices on other large, stagnant-lid regime  
61 planetary bodies.

62

63

### 64 **1. Introduction: steep-sided volcanic domes on Venus**

65

66 Of the terrestrial planets, Venus is the most similar to Earth in terms of size and density.  
67 However, on Venus there is no evidence for the global plate tectonic processes which  
68 dominate geological evolution on Earth. Instead, convective regime, crustal structure and  
69 volcanism on Venus are generally described by a 'thick stagnant lid' model, where a single  
70 plate of buoyant lithosphere inhibits mantle upwelling and active volcanism (Solomatov and  
71 Moresi, 1996). Volcanic activity within this convective regime can be assumed to relate mainly  
72 to plume-type upwellings, i.e. thermal anomalies inducing mantle melting beneath, and  
73 periodic puncturing of, the stagnant lid. Due to surface conditions which preclude the presence  
74 of liquid water or ice, Venus is a volcanic planet, with 75% of its surface interpreted to be  
75 primary volcanics, and 25% categorised as tectonic, i.e. volcanic origin but reworked by  
76 tectonics (Kaula, 1990). Geochemical data from Venus is limited, with 3 sites from the Venera-  
77 Vega landers returning detailed major element components of Venusian soil (Basilevsky,  
78 1997). Compositions are similar to terrestrial basalts, from which it is inferred that Venus has  
79 a similar bulk silicate composition to the Earth, although compositions do have elevated MgO,  
80 suggestive of higher mantle melt fractions (Ivanov, 2015). More silica-rich melt compositions  
81 on Venus would require either extensive fractionation of primary (basaltic) mantle melts, or in

82 the absence of subduction-related and/or hydrous mantle melting, some process involving re-  
83 melting of a Venusian crust that was already silica-enriched.

84

85 The surface of Venus is dominated by volcanic landforms (Saunders et al., 1991). Most  
86 volcanism is shield-type, with low angle slopes, most likely formed by effusive, basaltic  
87 volcanism (Crumpler et al., 1997; Ivanov, 2015; Kaula, 1990). The main Venusian landforms  
88 can be divided based on their morphological features (e.g. Tanaka et al. 1997), the principal  
89 ones being: shield plains, regional plains, lobate plains, tesserae and steep-sided domes  
90 (Ivanov, 2015). Shield plains make up 18.5% of Venus' surface (Hansen, 2005), and are  
91 generally similar in morphology, suggesting a common formation process. They are typically  
92 associated with small domes interpreted as monogenetic volcanoes formed at the same time  
93 as the shield plains (Guest et al., 1992; Ivanov, 2015). Regional plains make up approximately  
94 40% of the surface and may be identified in some instances as lava flows extending dozens  
95 to hundreds of kilometres, related to large volcanic centres (Ivanov, 2015). Shield, regional  
96 and lobate plains are all easiest to ascribe as the result of effusive volcanism and varying  
97 amounts of tectonic deformation. These landforms are consistent with eruption of large  
98 volumes of basaltic lava, which, under the high temperature, high pressure conditions of the  
99 Venusian surface (average surface temperature of 462°C, and a surface pressure equivalent  
100 to a 1 km water column on Earth) can flow very considerable distances.

101

102 Tesserae differ significantly from the other landforms in that they are equant or slightly  
103 elongate massifs, characterised by ridges and grooves. Tesserae make up approximately 8%  
104 of Venus' surface and are the most tectonically deformed regions of Venus, although likely  
105 were also initially produced by effusive volcanism (Ivanov and Head, 2015). The only landform  
106 present on Venus that does not fit with the observations of low-silica, effusive volcanism are  
107 steep-sided domes, sometimes named 'pancake' domes. Steep-sided domes are unusual in  
108 that their morphology implies eruption of more viscous lava, or a markedly different eruption  
109 style (see Ivanov and Head, 1999, for a summary). These volcanic landforms often occur in  
110 lineations or clusters and have characteristically rounded shapes in plan-view, flat tops, clearly  
111 pronounced frontal scarps, high elevations (few hundred metres), radial fracture patterns, and  
112 sometimes, small volcanic craters and auxiliary necks (Ivanov and Head, 1999). They are on  
113 average 20 km in diameter but reach up to 60 km, and have volumes usually exceeding 100  
114 km<sup>3</sup>. Two thirds of steep-sided domes are spatially and stratigraphically related to shield plains  
115 (Ivanov and Head, 1999; Ivanov, 2015), with domes overlying, or partially embayed by lava  
116 flows. These observations have resulted in a variety of explanations for the elevated viscosity  
117 of the domes required to produce the steep sides.

118

119 Based in part on evidence for a basalt-dominated surface, comparisons were initially drawn  
120 between steep-sided domes and seamounts on Earth (Bridges, 1995). Subsequent statistical  
121 analysis showed that there is only morphological similarity between smaller seamounts and  
122 steep-sided domes (Smith, 1996). Larger seamounts tend towards more traditional 'pointed  
123 top' shapes, and diverge markedly from the pancake dome shape, which has characteristically  
124 flat top surfaces across all sizes of dome. This suggests a fundamental difference between  
125 steep-sided domes on Venus and seafloor volcanoes on Earth, possibly due to differences in  
126 magma composition and crystallinity, but also possibly due to magma volume, effusion rate,  
127 cooling rate, and/or the pre-existing topography (Smith, 1996). Alternatively, it has been  
128 suggested that steep-sided domes more closely resemble terrestrial rhyolitic domes. Fink et  
129 al. (1993) suggested that dome emplacement on Venus is consistent with a melt of similar  
130 viscosity to terrestrial rhyolite. Modelled cooling times, based on a constant volume theoretical  
131 approach to dome relaxation, return emplacement timescales of 650-7400 years (McKenzie  
132 et al., 1992), also implying lava viscosities and temperatures consistent with a rhyolitic

133 composition. Geochemical modelling of the Venera-Vega lander compositions shows that  
134 rhyolite compositions can be produced by considerable fractionation of Venusian basalts  
135 (Shellnutt, 2018, 2013). Ivanov and Head (1999) instead suggested that the juxtaposition of  
136 steep-sided domes with basaltic terrains is more consistent with genesis of rhyolitic magma  
137 by crustal remelting associated with upwelling plumes. However, the re-melted crust would  
138 have to have been non-basaltic, and possibly granitic in composition to begin with, creating  
139 an additional quandary. Any model where rhyolitic domes are generated by plume-induced re-  
140 melting of the crust or extensive fractionation of basalt would also imply that domes should be  
141 more common than they are (Ivanov, 2015); instead, the relative rarity of these domes implies  
142 that they are formed via an unusual set of conditions. Eruption of rhyolitic magma might also  
143 be inconsistent with primary observations made on the steep-sided domes. The domes are  
144 characterised by smooth upper surfaces and only show signs of late-stage fractures (Stofan  
145 et al., 2000; Plaut et al., 2004). Stofan et al. (2000) calculated that for present surface  
146 conditions, rhyolitic lavas should quickly form thick crusts, ultimately resulting in a much  
147 blockier dome morphology than observed. Much higher surface temperature conditions would  
148 be required to prevent rhyolitic lavas forming distinct blocky, fractured dome surfaces  
149 (Anderson et al., 1998; Stofan et al., 2000). Comparison with radar properties of terrestrial  
150 silicic lava domes supports the assertion that Magellan data is instead consistent with a less  
151 evolved dome lava composition. In addition, Stofan et al. (2000) noted that depressions in the  
152 upper surfaces of some steep-sided domes imply more fluid dome interiors, again suggestive  
153 of a basaltic lava composition.

154  
155 Alternative explanations for the elevated viscosity of dome-forming magmas include higher  
156 levels of crystallinity (e.g. Sakimoto and Zuber, 1995), or a magma rich in gas bubbles (Pavri  
157 et al., 1992), although a non-rhyolitic, volatile-rich magma seems unlikely, due to dominance  
158 of low viscosity, basaltic lava flows on Venus. Gregg and Fink (1996) and Bridges (1997) also  
159 took into account the sluggish character of basaltic eruptions due to the much greater  
160 atmospheric pressure and temperature on Venus than on Earth. Analysis of the ambient  
161 effects on basalts vs. rhyolites under Venusian and Earth-like conditions supports a basaltic  
162 composition for Venusian steep-sided domes (Bridges, 1997) consistent with the cooling  
163 models of Stofan et al. (2000). In addition, more recent mathematical modelling on dome  
164 emplacement (Quick et al., 2016) using a time-variable volume approach has shown that  
165 emplacement times are a lot quicker (2-16 years) than previous estimates (McKenzie et al.,  
166 1992), consistent with a basaltic-andesitic composition magma. However, a fundamental  
167 problem with invoking a basaltic or andesitic lava source for steep-sided domes is the obvious,  
168 distinct contrast in morphology between domes and surrounded volcanic terrains. It is not clear  
169 how a change in volatile content or crystal content could result in such a clear transition in  
170 eruptive style, without producing a range of intermediate landforms. Similarly, steep-sided  
171 domes are intimately related with basaltic terrains, suggesting that the two volcanic landforms  
172 are connected, but domes are comparatively rare, implying that the mechanism(s) forming  
173 them are somewhat anomalous. As such, despite observed inconsistencies between steep-  
174 sided domes and features formed by high-viscosity, rhyolitic lavas (Stofan et al., 2000) a full  
175 explanation of the morphology of steep-sided domes, especially the stark contrast to the  
176 extensive shield plains with which they are associated, remains elusive.

177  
178 Here we propose an alternative model for the formation of steep-sided volcanic domes which  
179 accounts for many of their observed features, but which also circumvents clear issues with  
180 advocating eruption of basaltic or rhyolitic lava. Based on field observations near Marki,  
181 Cyprus, we propose that these volcanic domes form by extrusion of crystal mush. As such,  
182 we propose that they share a common magmatic origin with basaltic terrains on Venus, but  
183 form by a fundamentally different extrusive process.

184  
185  
186  
187  
188  
189  
190  
191  
192  
193  
194  
195  
196  
197  
198  
199  
200  
201  
202  
203  
204  
205  
206  
207  
208  
209  
210  
211  
212  
213  
214  
215  
216  
217  
218  
219  
220  
221  
222  
223  
224  
225  
226  
227  
228  
229  
230  
231  
232  
233  
234

## **2. Marki: picritic domes within the Troodos ophiolite**

The Troodos Massif, which forms one of the main tectonic units comprising the island of Cyprus in the Eastern Mediterranean, is an Upper Cretaceous age ophiolite formed in the Tethyan Ocean around 93-90 Ma (Mukasa and Ludden, 1987). The Troodos Massif is one of the most fully documented ophiolites in the world, and has been pivotal in aiding development of theories on plate tectonics and sea-floor spreading, and magmatic-tectonic-hydrothermal process associated with the formation of oceanic crust (Robertson, 2004). Results of mapping and scientific drilling allow a pseudo-stratigraphy of the main Troodos ophiolitic body to be constructed, consisting of a sequence of serpentinised harzburgite and ultramafic cumulates, overlain by layered and then massive gabbros, a sheeted dyke complex, and extrusive volcanic sequence including overlying volcanoclastic sediment (Dilek and Furnes, 2009; Gass, 1968). The extrusive volcanic sequence can be further divided into a lower basal unit (transitioning downwards into the sheeted dyke complex), and both lower pillow lava (LPL) and upper pillow lava (UPL) units. Differences in appearance allow LPL and UPL to be mapped in the field, although there are also important geochemical differences between the 2 units which have resulted in various theories for the tectonic setting in which the Troodos Ophiolite formed (e.g. Pearce and Robinson, 2010). Most likely, the Troodos complex formed in an extensional oceanic regime, either a back-arc or early fore-arc environment, with variable input from an incipient subduction system, evident from a marked boninitic signature in the UPL unit (Woelki et al., 2018).

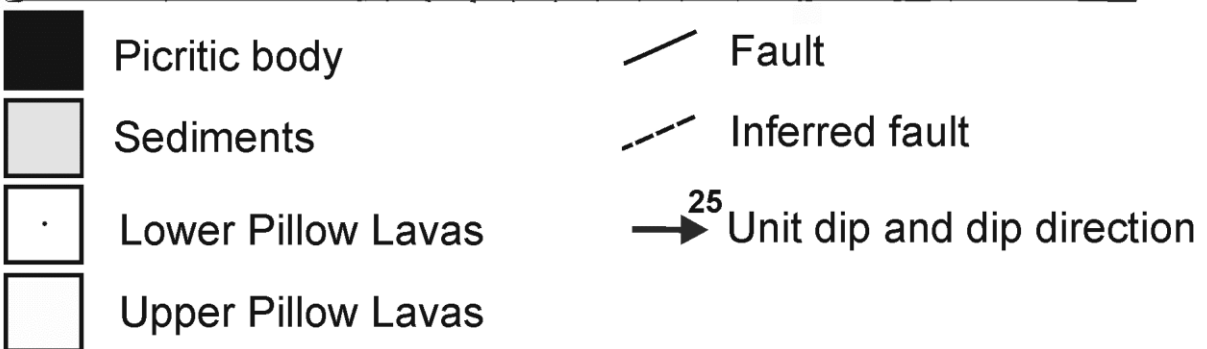
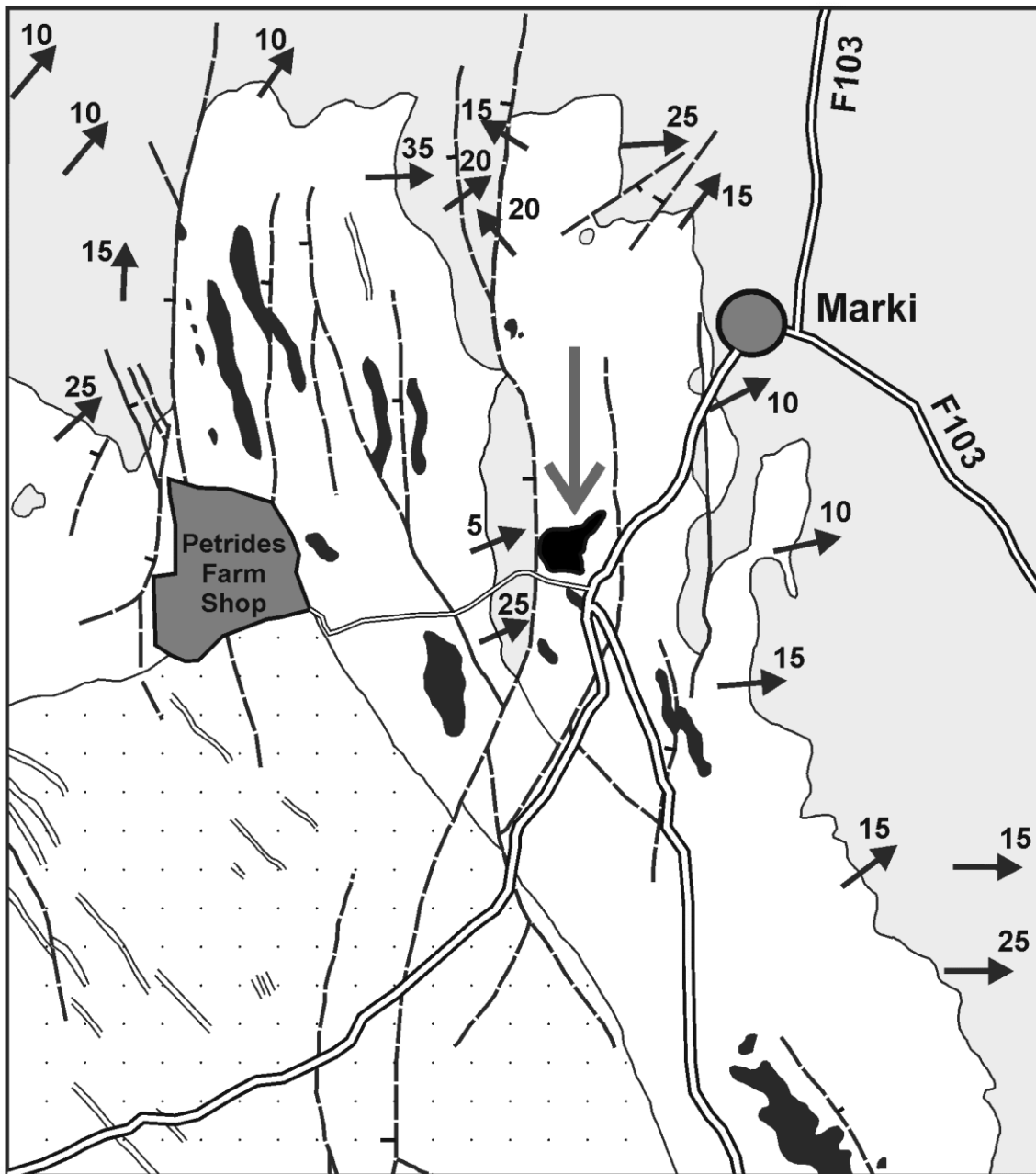
UPLs are generally silica-undersaturated, often olivine-bearing basalts. Occasionally, more ultramafic, olivine-rich varieties occur towards the top of the UPL sequence (Malpas and Langdon, 1984). These picritic basalts and ultramafic rocks of the UPL were originally documented by Gass (1958) and Searle and Vokes (1969), and described as varying from shallow intrusive to extrusive. In the area adjacent to the village of Marki (or Margi), approximately 50 km SW from Nicosia, on the northern flank of the Troodos, small ultrabasic lava flows and picritic pillows and flows occur within the UPL. Olivines within these members are typically highly forsteritic (~Fo92) (Gass, 1958; Searle and Vokes, 1969). Malpas and Langdon (1984) noted that the position of ultramafic rocks near the top of the pillow-lava sequence suggests that they were extruded late-stage. They further noted that major element bulk rock chemistry and phenocryst composition demonstrated that removal or addition of olivine phenocrysts can account for the full compositional range of UPL members, following derivation from a basaltic parental magma. As such, olivine-rich members of the UPL were inferred to represent crystal-rich magmas formed from the same magmatic system which fed the entire UPL unit. Gass (1958) viewed olivine-rich picritic and ultramafic bodies in this region as representing both shallow intrusive and extrusive bodies. However, in contrast to the classification of Gass (1958), field relations of larger picritic bodies within this area provide robust evidence that they represent repeated extrusion of viscous, crystal-rich mush of ultramafic to mafic bulk composition, onto the seafloor via an unusual, fault-controlled mechanism. This same mechanism may provide insight into formation of steep-sided volcanic domes on Venus.

## **3. Field observations and petrology of a Marki picritic body**

The region around Marki contains numerous discrete picritic bodies, as shown in Figure 1, based on original mapping and classification by Gass (1958). One of the largest and most prominent of these, 'Picrite Hill' is marked in Figure 1. This body sits on top of lavas of the

235 UPL unit, marked by a shallow angle contact, and adjacent to a N-S trending extensional  
236 fault. Highly localised accumulation of 10s of meters of volcanoclastic sediment adjacent to  
237 this fault is characteristic of lava/umber relations in the UPL regionally (Constantinou and  
238 Govett, 1973; Robertson and Hudson, 1973), and implies that the fault was active during the  
239 Cretaceous, forming a half-graben in which sediments accumulated. From Figure 1 it is also  
240 apparent that all substantial picritic bodies within the Marki region occur adjacent to  
241 extensional faults.  
242

300m

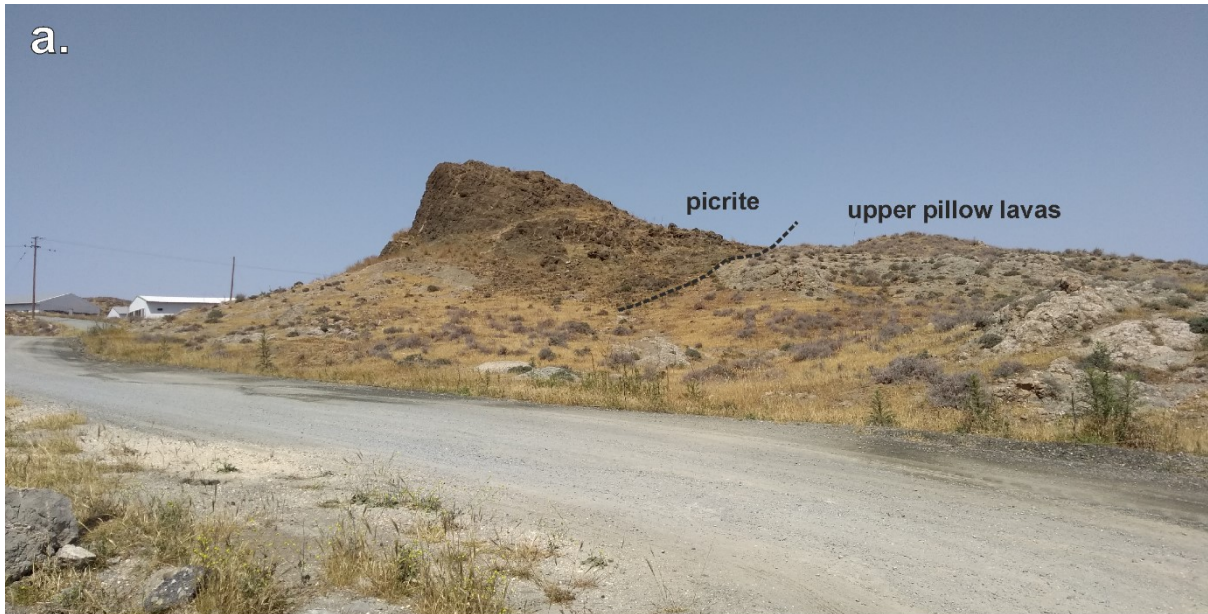


243  
244  
245  
246  
247

**Figure 1.** Sketch geological map showing picritic volcanic bodies near Marki, Cyprus, adapted from Gass (1958). Large grey arrow marks Picrite Hill.

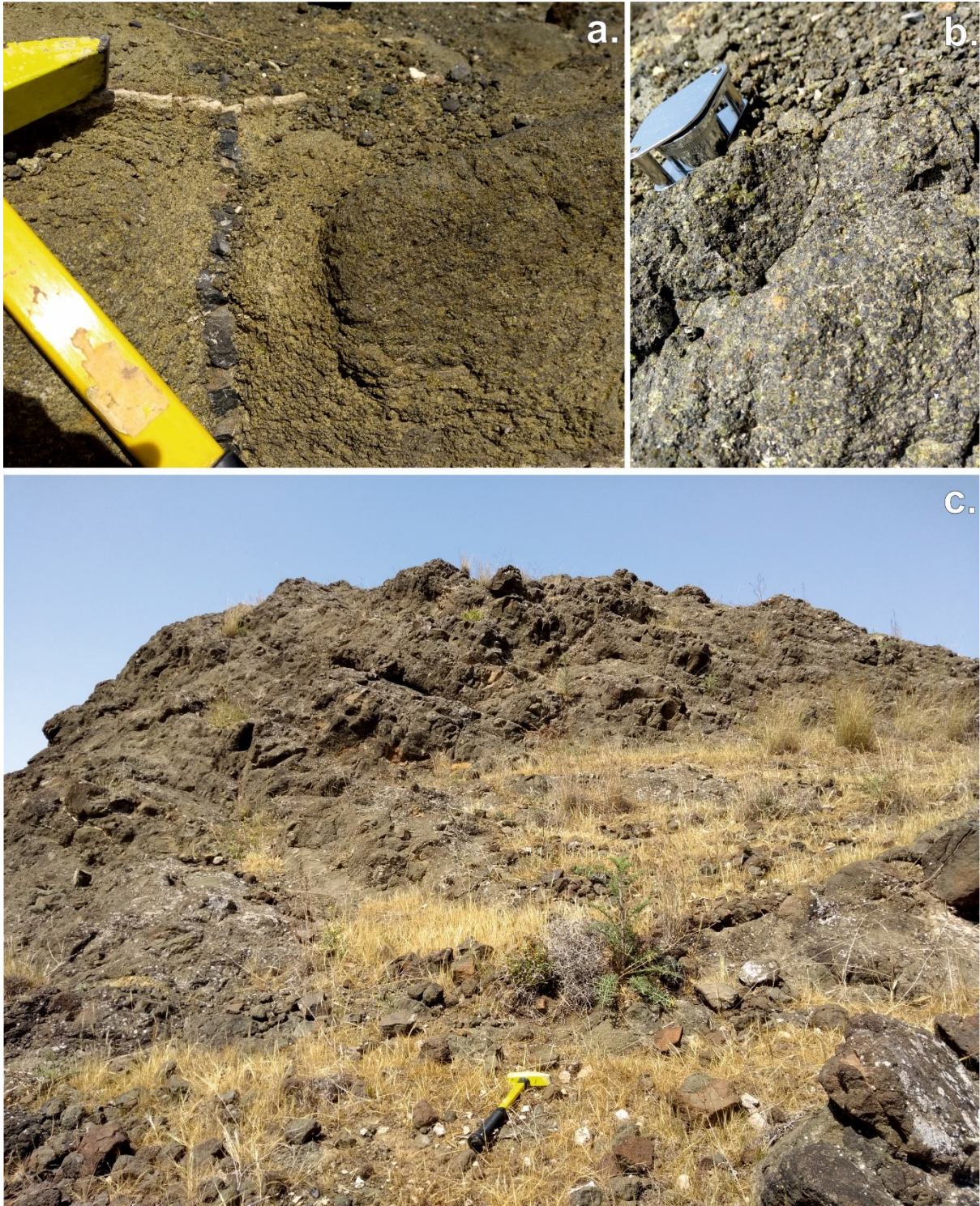


248 Picrite Hill is an approximately 50m diameter body with a tongue extending an additional  
249 40m to the NE. The body rises to a prominent topographic high towards the SW,  
250 approximately 25-30m above the underlying UPL pillow lava basement (Figure 2). This  
251 central, plug-like portion of the body is massive at the base, but grades upwards into a series  
252 of distinct, meter-scale units dipping around 30-35° to the NE (Figures 3), supporting a steep  
253 edifice (Figure 2a,b). Towards the top of the body, weak columnar jointing is also evident.  
254 The picrite has a uniform, brown appearance in the field which differentiates it from the  
255 underlying, grey UPL pillowed terrain, and contains up to 8mm diameter, bright green olivine  
256 phenocrysts (Figures 2a, 3a,b). Olivine content varies between units, exceeding 50% by  
257 volume in places. Individual units towards the top of the body can be traced laterally, and  
258 variably thin towards the NE. This is consistent with elongation of the body in the same  
259 direction. The NE elongation of Picrite Hill consists of thinner, interlayered units of lower-  
260 crystallinity. Underlying UPLs show a similar, although much lower angle tilt to the NE of 5-  
261 10° locally, and up to 30° regionally. As such, field evidence indicates that Picrite Hill  
262 consists of interlayered, crystal-rich lavas (>50% in places), with more mobile, runnier lavas  
263 (phenocryst contents 30%+), repeatedly erupted onto a shallow palaeoslope on the Upper  
264 Cretaceous, pillowed basaltic sea-floor. More elongate picritic bodies in the surrounding area  
265 indicate that elsewhere, picritic lavas accumulated in half-grabens on a seafloor which was  
266 more faulted and steeply dipping. Poorly-developed slickenslide surfaces on the southern  
267 margin of Picrite Hill indicate that the entire body moved downslope, with less viscous lavas  
268 flowing further, forming a slight elongation. The body was clearly extruded in a series of  
269 events, although poorly developed columnar jointing towards the top of the body indicates  
270 relatively quiescent conditions, and minimal flow of crystal-rich lavas. The blockier lower  
271 parts of the body, and some units with better developed columnar jointing, may have formed  
272 by intrusion of crystal-rich magma into the base of the edifice. Subsequently, the body,  
273 especially lowermost units, were cut by various basaltic dykelets (Figure 3a), most likely  
274 formed from late-stage fluids squeezed from the body as it cooled. These, in turn, are cross-  
275 cut by later, hydrothermal carbonate and zeolite-filled veins.  
276



277  
 278  
 279  
 280  
 281  
 282  
 283  
 284

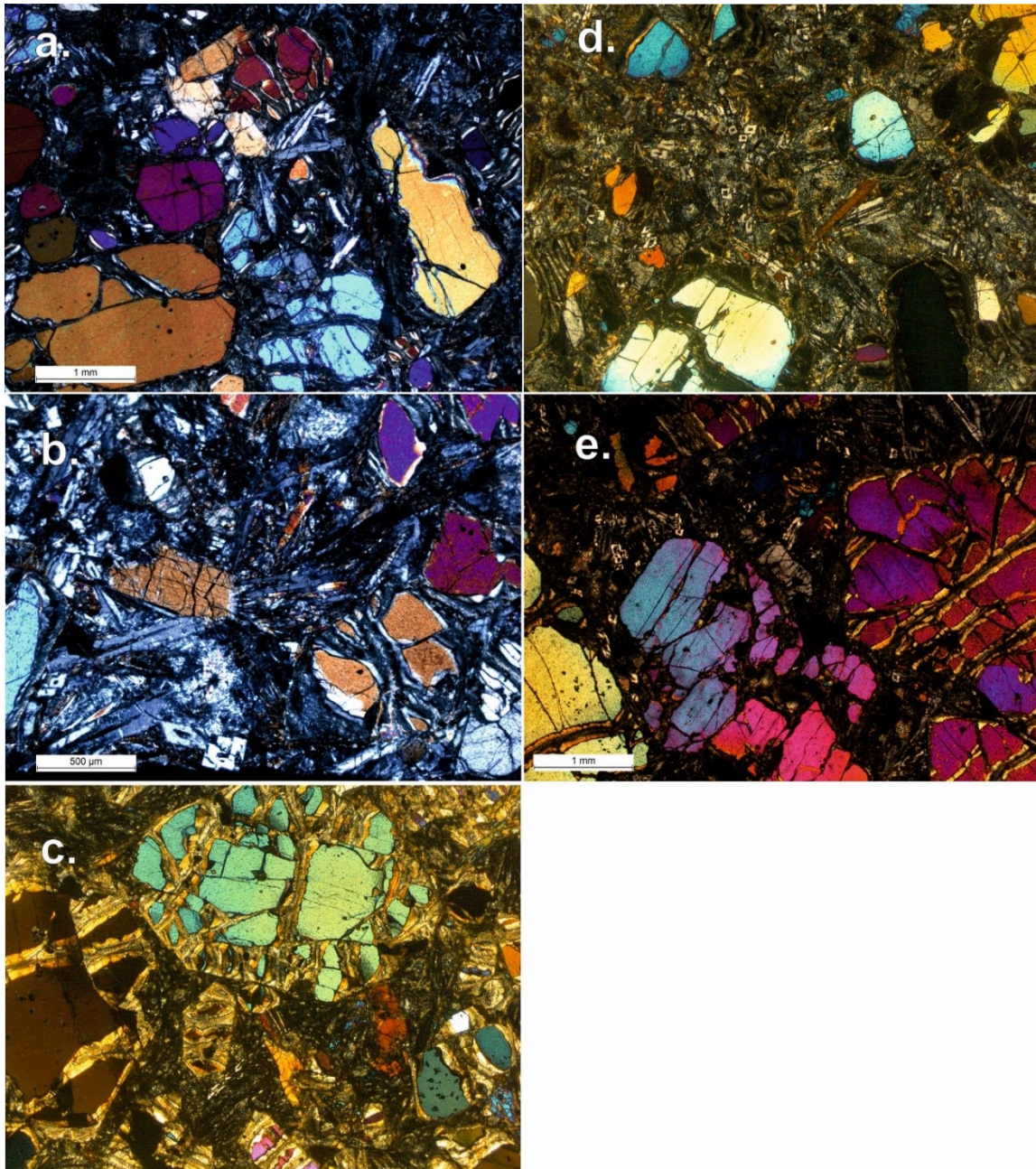
**Figure 2** (COLOUR). Photos of Picrite Hill a) Looking WNW showing distinction between picrite and the underlying upper pillow lavas; b) looking E, where individual units are more easily discerned, some extending and thinning to the NE. The entire body can be viewed as interlayered viscous crystal mush with runnier lavas, with a low-angle contact with underlying Upper Pillow Lavas.



285  
286  
287  
288  
289  
290  
291  
292  
293  
294  
295

**Figure 3** (COLOUR). a) Margins of the body are cut by basaltic dykelets (dark), representing late-stage fluids being squeezed out of the crystal mush, cross cut by later carbonate veins (white); b) crystal-rich unit in the central, more massive centre of the body showing typical appearance of the picrite. c). Photo of the SW portion of the body (looking approx.. N), showing transition from more massive to more layered units vertically upward, development of columnar jointing towards the top of the body, and the general 30°+ dip of the layers to the NE.

296 Sampling and petrographic analysis reveal variations in phenocryst content and groundmass  
297 between units, but also considerable internal variation within some units. All units are picritic,  
298 consisting of large, euhedral and sometimes euhedral-to-subhedral mm-sized phenocrysts of  
299 olivine, variably altered to serpentine, and some smaller, but again up to mm-sized,  
300 phenocrysts of augitic clinopyroxene. Groundmass is variable between units, and in some  
301 cases within thin sections from the same unit. In accordance with Malpas and Langdon  
302 (1984), picrites can be subdivided as vitrophyric and holocrystalline (Figure 4). Vitrophyric  
303 picrites are dominated by the presence of large (up to 8 mm sized) phenocrysts of olivine,  
304 ranging up to 50-60% by volume, set in a fine-grained to glassy groundmass, now  
305 extensively serpentinised. Olivine phenocrysts are unzoned, generally euhedral, sometimes  
306 exhibiting a weak cleavage, but with some slightly corroded boundaries. As noted by Gass  
307 (1958), olivines are highly forsteritic (Fo92). Clinopyroxene phenocrysts are much less  
308 abundant and generally small, although ranging up to 2 mm sized. Some acicular  
309 clinopyroxene is also noted. Holocrystalline picrites have groundmasses with variable grain  
310 size. The proportion of olivine phenocrysts is generally lower (40-50%) and olivine is  
311 generally slightly smaller and more extensively serpentinised. The groundmass in these  
312 units largely comprises plagioclase microlaths, intergrown with clinopyroxene and euhedral  
313 magnetite, and some rare orthopyroxene. In places the groundmass plagioclase can be  
314 relatively coarse, with laths ranging up to 0.5mm and better described as microphenocrysts.  
315 Some samples are, however, transitional between both types, with groundmass being  
316 relatively coarse grained in places, and fine-grained and/or extensively serpentinised in other  
317 places, even within the same thin section. As such, petrographic investigation reveals that  
318 the body is internally chaotic and highly laterally and vertically variable, as expected from a  
319 volcanic edifice formed by multiple events. Phenocryst content of most samples implies that  
320 flow under surface conditions would be very limited, consistent with field observations which  
321 indicate flow of a few 10s of meters even for the most crystal-poor lavas. Composition of all  
322 samples, especially the abundance of unzoned, forsteritic olivine, and the basaltic  
323 composition groundmass, is consistent with picrites representing a crystal mush, tapped  
324 from magma chambers. Close association of picrites with underlying UPL units is consistent  
325 with a common origin, where relatively primitive UPL magmas formed by small degrees of  
326 fractionation of olivine and minor clinopyroxene from a basaltic parent, and picrites represent  
327 the cognate olivine-rich mush extruded, later on, from the same magmatic system following  
328 a prolonged period of fractionation, UPL eruption and rejuvenation of magmatic systems by  
329 primitive melt.  
330  
331  
332



333  
334

335 **Figure 4 (COLOUR).** Photomicrographs of Marki picrite. (a) and (b) are from the same  
 336 'holocrystalline picrite' unit, after the classification of (Malpas and Langdon, 1984), showing  
 337 large olivine and minor clinopyroxene phenocrysts, with varying alteration, in a finer-grained  
 338 basaltic groundmass, variably altered. In places, large plagioclase microlaths are noted in  
 339 the groundmass; in pockets within individual sections (b) the grain size groundmass  
 340 increases substantially, and large, radiating plagioclases are apparent. (c) 'Vitrophyric'  
 341 picrite. Extensive serpentinisation of large, euhedral olivines is variable, largely due here to  
 342 surface weathering. Minor, smaller clinopyroxene and plagioclase is also present.  
 343 Groundmass here is extensively serpentinised, although still glassy in places. (d) Same  
 344 section as (c) showing variability in groundmass and phenocryst content within samples.  
 345 Serpentinised groundmass here contains larger microlaths of plagioclase as well. (e) Other  
 346 'vitrophyric' picrite sections have phenocryst contents exceeding 50%, with large, euhedral,  
 347 interlocking olivine.

348

349 Phenocryst content of a number of units is close to, or exceeds 45-55%, the range of values  
350 over which eruption of a basaltic magma becomes unfeasible (Marsh, 1981), and implies an  
351 apparent magmatic viscosity between one and several orders of magnitude higher than a  
352 crystal-free magma (Champallier et al., 2008; Okumura et al., 2016). Development of weak  
353 columnar jointing and the limited lateral extent of more crystal-rich units suggest that they  
354 also did not flow significantly once erupted. Many units contain clusters of mm-sized,  
355 interlocking crystals of olivine, which would have inhibited flow, consistent with surface flow  
356 of a few meters at most. Flow of less viscous, lower crystal content lavas was a few 10s of  
357 meters. Therefore, picritic lavas were able to build a steep-sided volcanic edifice, in marked  
358 contrast to the extensive, relatively flat terrain of UPL pillows on which this, and other similar  
359 bodies, rest. The observation that all picrite bodies rest on the uppermost extrusive  
360 sequence is consistent with the inference of an extrusive origin, and implies that picrite was  
361 erupted as the final stage of magmatism. Marked differences in unit dip between picrite and  
362 UPL confirm that Picrite Hill formed as a steep-sided edifice, rather than having a current  
363 morphology imposed by secondary processes such as erosion. The association of picritic  
364 bodies with extensional faults provides an obvious mechanism for explaining how such  
365 crystal-rich magmas were erupted. Vertical extent of these faults, and degree of fault  
366 movement, are difficult to ascertain. However, throughout of the main body of the Troodos  
367 there is extensive evidence for propagation of extensional faults deep into the crustal  
368 sequence, with larger, detachment faults extending through extrusives and sheeted dyke  
369 units to the boundary of massive gabbros, i.e. extending to depths of deep crustal magma  
370 chambers (Dilek and Furnes, 2009). In the Troodos ophiolite there is also evidence for  
371 periods of crustal thinning through extension, during magmatically quiescent periods,  
372 resulting in detachment faulting and block movement throughout the ophiolitic sequence  
373 (Robertson and Xenophontos, 1997). The fault adjacent to Picrite Hill extends at least  
374 several hundreds of meters laterally, and is part of a series of approximately N-S trending  
375 faults on the northern flank of the Troodos which extend many km. In the Marki area,  
376 extensional faults are associated with locally thick deposits of volcanoclastic sediment,  
377 accumulated in half-grabens. A type example of the relationship of umbers with UPL pillows,  
378 which implies on-axis, fault-controlled hydrothermal discharge (Constantinou and Govett,  
379 1973), is found 100m W of Picrite Hill. As such, the fault with which Picrite Hill is associated  
380 likely propagated deep enough into the crust to tap parts of the magmatic system with which  
381 UPL units were derived. Extension on this fault would then have allowed viscous crystal  
382 mush within this magmatic system, accumulated during prolonged basaltic magmatism, to  
383 extrude onto the sea floor. Strong N-S alignment of faults within the Marki region means that  
384 many of the picritic bodies are lens shaped and elongated N-S. However, Picrite Hill,  
385 associated with one of the most extensive fault systems is, aside from elongation in one  
386 direction representing preferred flow, an approximately circular body with a clear, central  
387 complex. Absence of any basaltic units within the body suggests that this extrusion occurred  
388 after normal magmatism had ceased, although adjacent volcanoclastic sediment and an  
389 absence of any sedimentation implies that the process occurred shortly after formation of the  
390 main body of UPL within this area. Picrite Hill consists of multiple units, implying that  
391 formation of the body was episodic, possibly related to pulses of movement on the main  
392 feeder fault. Repeated opening of this fault during the final stages of crustal extension of the  
393 Troodos, and a large difference in pressure from the surface to the tapped magmatic  
394 system, would have allowed crystal mush to flow and extrude onto the seafloor. The highly  
395 non-Newtonian nature of this viscous crystal mush explains why it could be extruded onto  
396 the seafloor from deep within the crust due to a large pressure differential, but would then  
397 only flow limited distances once on the surface (e.g. Champallier et al., 2008; Okumura et  
398 al., 2016). Coarser groundmass within some units is consistent with eruptions of crystal  
399 mush into, or associated with, a hot lava pile, and relatively rapid formation of the body.

400 Lower parts of the body might have formed, later on, by injection of mush into the bottom of  
401 a lava pile.

402

#### 403 **4. Extrusion of crystal mush on Venus**

404

405 An interesting observation of the Marki region is the juxtaposition of two contrasting volcanic  
406 landforms: pillowed and sheet-like basaltic lava flows of the UPL overlain by steeper picritic  
407 volcanic domes and lenses. All observations imply that picritic bodies and basaltic terrains  
408 share a common origin, with picrite formed by extrusion of crystal mush from the same  
409 magmatic system in which UPL basalts evolved. This observation is consistent with the  
410 variable modal, forsteritic olivine content of UPL basalts (Gass, 1958). The high olivine  
411 content of picrites means that they are classified as ultramafic bodies, in contrast to basaltic  
412 (mafic) pillows, although it is solely the extreme difference in crystal content, and possibly a  
413 small difference in volatile content, which explains the marked contrast in eruption style.  
414 Considerable extensional faulting within the Troodos must have been required to extrude  
415 this picritic crystal mush, which would otherwise have remained trapped within the crust. The  
416 presence of unzoned, highly forsteritic olivine with only minor clinopyroxene implies that this  
417 mush likely formed in a relatively high temperature, and therefore relatively deep, magmatic  
418 system.

419

420 A similar, although much larger scale process of crystal mush extrusion could be invoked to  
421 explain the formation of steep-sided volcanic domes on Venus. In the proposed model, small  
422 degrees of fractionation of mantle-derived basaltic melt takes place within extensive  
423 magmatic systems in the Venusian crust. Over prolonged periods of time, periodic eruption  
424 of basaltic lava and reinjection of primitive magma into the magmatic system results in  
425 substantial accumulation of crystal mush, perhaps analogous to extensive ultramafic  
426 cumulate sequences typical of terrestrial ophiolitic sequences. During magmatically  
427 quiescent periods there is no new input of magma into the crust, and effusive volcanism  
428 ceases. Extensional faulting provides a mechanism for allowing accumulated crystal mush  
429 within this magmatic system to extrude onto the surface. The high crystal content of this  
430 mush results in a markedly different volcanic landform, steep-sided domes, in contrast to  
431 underlying basaltic terrains. At a later stage, renewed magmatic input would result in a return  
432 to effusive type basaltic eruptions.

433

434 This model can account for a number of observed characteristics of steep-sided volcanic  
435 domes. (1) Firstly, it readily explains the intimate association of steep-sided domes with  
436 basaltic terrains, especially extensive lava flows and coronae, on Venus. Crystal mush would  
437 be formed at depth during the prolonged, high temperature, low-degree fractionation of  
438 basaltic magma inferred for large-scale Venusian volcanism. This mush is then parental to  
439 the volcanic domes. The same magmatic process explains formation of various volcanic  
440 terrains and volcanic domes, explaining their close association without needing to invoke a  
441 contrasting magmatic processes. (2) Extrusion of crystal mush can only occur during  
442 magmatically quiet periods. This is consistent with observed clustering of steep-sided domes  
443 at certain stratigraphic heights within volcanic terrains (Ivanov and Head, 1999). However,  
444 unlike other proposed mechanisms, dome formation by mush extrusion could occur at any  
445 point during more widespread basaltic volcanism, explaining why domes are sometimes  
446 partly embayed or covered by flows following renewed basaltic magmatism. (3) At the same  
447 time, high crystal contents of mush explain why steeper domes are supported on the high  
448 temperature, high-pressure Venusian surface, and why there is a marked contrast in  
449 morphology between domes and lava flows. (4) The process of mush extrusion is unusual,  
450 and dependent on both cessation in normal magmatism and extensional faulting, which

451 would explain why domes have unique characteristics and why there is not, instead, a  
452 gradual transition from lava flows or shield terrains to steep-sided domes. (5) However,  
453 extrusion of mafic to ultramafic mush would explain the flatter, more rounded-top  
454 morphology of volcanic domes on Venus, in contrast to the blockier texture expected with  
455 eruption of more rhyolitic lava. Prolonged eruptions of mush through the same fault system  
456 would, presumably, eventually mainly occur through injection into the base of volcanic piles,  
457 consistent with many observations. However, piles could also accumulate through repeated  
458 eruptions and build-up of lava flows. (6) As eruptions of mush are fault-controlled this model  
459 also explains why steep-sided domes on Venus are not ubiquitous, but instead, rather  
460 unusual features. (7) Extrusion of mush would explain why Radar properties of the domes  
461 are similar to those of surrounding lava fields (Ford, 1994; Stofan et al., 2000), and finally,  
462 (8) extrusion of crystal mush would also be consistent with a single phase of eruption, or  
463 pulsed/episodic emplacement of domes that has been inferred by some authors based on  
464 observed aspect ratios (Fink et al., 1993; Pavri et al., 1992).

465  
466 However, it is important to note that picritic extrusions in Cyprus only indicate a possible  
467 mechanism for formation of volcanic domes on Venus, rather than providing a terrestrial  
468 analogue. There are clear differences between picritic bodies at Margi and Venusian  
469 volcanic domes in terms of (1) scale of eruptions and magma volumes, (2) the external  
470 shape of bodies (circular vs elongate), (3) the tectonic regime in which volcanic bodies  
471 occur, and (4) the contrasting extent of weathering and consequent modification in dome  
472 morphology on Earth. Landforms around Marki are small bodies less than 100 meters in  
473 diameter. Most bodies are also elongate and not circular. In terms of dimensions, therefore,  
474 Venusian steep-sided domes are 3 to 4 orders of magnitude larger than any feature noted in  
475 the Marki region. However, the scale of volcanic activity on Venus associated with shield and  
476 lava flow terrains is similarly orders of magnitude larger than that associated with oceanic  
477 crust formation in the Troodos massif. Importantly, the relative extent of dome-related  
478 volcanism on Venus is not inconsistent with the vast scale of magmatism recorded by  
479 extensive lava flows and shield terrains. This is demonstrated by using a simple mass  
480 balance calculation to determine the volume of basaltic magma required to produce Picrite  
481 Hill. The volume of basaltic magma required to fractionate the volume of Fo92 crystals  
482 present in a 25m high hemispherical dome with a crystal fraction of 0.5, corresponds to an  
483 erupted basaltic lava flow 1m thick and roughly 1 km in diameter. Scaling this to a 20km  
484 steep-sided dome implies an erupted basaltic lava flow of 10m thick and 700 km diameter.  
485 Given the large uncertainties with this type of calculation, the scale of dome size to extent of  
486 basaltic volcanism for both Marki and Venus are, to a first approximation, reasonable.

487  
488 A similar scale issue occurs when attempting to find other terrestrial analogues for Venusian  
489 volcanic domes. Pavri et al. (1992) noted that Venusian domes are typically 2-3 orders of  
490 magnitude larger than terrestrial rhyolitic domes, although also noted that association of  
491 domes with coronae, and the probability that magmatic reservoirs on Venus would, due to  
492 the absence of plate motion, grow to unusually large sizes, could be used to invoke a model  
493 for dome formation from rhyolitic magma following fractionation of basaltic parental melt.  
494 Similarly, association of domes with extensive magmatic terrains and large-scale  
495 fractionation of basalt can also be used, here, to invoke volumetric extrusion of crystal mush.  
496 The contrasting nature of plate tectonic vs stagnant lid regimes on Earth and Venus, in  
497 tandem with strongly contrasting surface conditions, suggest that the search for true  
498 terrestrial analogues for all volcanic landforms is of limited value. However, it is also possible  
499 that smaller mush-type eruptions occur on the Venusian surface. Hansen (2005) used  
500 Magellan data to conducted detailed geological mapping on Venus. This work identified  
501 numerous small shield and shield-like features distinct from extensive lowland lava flows in



502 which they are found. Hansen (2005) considered the possibility that these features represent  
503 some type of point-source partial re-melting of the highland crust. They could, alternatively,  
504 represent smaller scale extrusion of basaltic crystal mush.

505

506 Most picritic bodies near Marki are elongate. However, most elongate bodies are small,  
507 some likely representing single eruptions (Gass, 1958). The much more substantial Picrite  
508 Hill is an approximately circular body, with an elongate tongue formed by limited preferential  
509 flow of less viscous lavas in one direction. Extrusion of material onto a gently-sloping  
510 seafloor, consistent with the low-angle contact between picrite and UPL, explains the  
511 observed shape of the body. Elsewhere in this area, a highly-faulted and tilted palaeo-  
512 seafloor consisting of a series of half-graben accounts for the shape of picritic bodies. Large  
513 extensional faults in the Marki region have a strong N-S trend, consistent with the regional  
514 spreading direction of the main Troodos body (Robertson and Xenophontos, 1997). It is  
515 generally agreed that the Troodos Ophiolite formed in a Supra-Subduction Zone  
516 environment, with extension due to subduction initiation and/or back-arc spreading (Pearce  
517 and Robinson, 2010). The nature of faulting within the Troodos body, and at Marki  
518 specifically, has controlled the morphology of picritic extrusions to a significant degree.  
519 Differences in local and planet-wide magmatic-tectonic regime on Venus (Ivanov, 2015;  
520 Ivanov and Head, 2011), surface conditions, scale of eruption, and mechanical response of  
521 the crust and dyke propagation (Foster and Nimmo, 1996; Karato and Barbot, 2018; Mikhail  
522 and Heap, 2017) could easily result in fundamental differences in morphology of volcanic  
523 landforms.

524

525 Extrusion of crystal mush at Marki is facilitated by extensional faulting related to seafloor  
526 spreading after normal magmatic processes ended. The absence of a comparable  
527 mechanism on Venus would, therefore, necessitate some alternative process to induce  
528 fracturing and faulting of the Venusian crust. Extensional faulting has been inferred for other  
529 parts of Venus. Rift-like valleys within the Aphrodite Terra can be traced for 1000s km in  
530 some instances, and elsewhere, extensional tectonism has produced marked belts of  
531 deformation, persisting over 100s of km (Ivanov and Head, 2011). However, although a  
532 correlation between rifting and coronae, and large-scale volcanism generally, has been  
533 noted, volcanic domes on Venus have no discernible relationship with such this type of  
534 large-scale rifting (Airey et al., 2017). Large-scale rifting on Venus is often assumed to result  
535 from crustal doming associated with upwelling plumes (Ivanov and Head, 2015), which  
536 explains a correlation with extensive, i.e. basaltic, volcanism. As such, volcanic domes  
537 formed by extrusion of crystal mush might be expected to post-date such rifting, or be  
538 associated with a smaller scale extensional process. Instead, correlation of domes with  
539 coronae and other similar magmatic landforms, and associated with extensive basaltic  
540 terrains, suggests that domes could be associated with smaller scale faulting to shallow  
541 magmatic systems. Significant differences in crustal strength between Venus and Earth (e.g.  
542 Karato and Barbot, 2018; Mikhail and Heap, 2017) should result in a significant deflection of  
543 the brittle-ductile transition to much shallower levels in the hotter, Venusian crust. As such,  
544 there will be fundamental differences in emplacement of bodies of magma, supporting the  
545 presence of magma chambers at comparatively higher levels in the Venusian crust. For  
546 example, Mikhail and Heap (2017) invoked a model where large bodies of magma  
547 associated with coronae are emplaced at high levels in the Venusian crust via diapirism, due  
548 to the inhibition of fracture propagation and dyke emplacement. Magma chambers feeding  
549 the volcanic plains with which steep-sided domes are associated could, therefore, be at  
550 comparatively shallow depths in the hotter, more ductile Venusian crust, meaning that  
551 extensional faults required to tap them would be smaller scale features.

552

553 Whether steep-sided domes are associated with smaller-scale extensional faulting is not  
554 clear. Domes often have surfaces cut by radial and/or concentric fractures, although these  
555 can readily be explained by fracturing of cool, solid rinds (Ivanov, 2015; Pavri et al., 1992).  
556 However, other observations of steep-sided volcanic domes are consistent with a fault  
557 controlled extrusion process. The notable dome cluster near Alpha Regio, for example,  
558 consists of 7 partially overlapping domes with a strong E-W trend, associated with a series of  
559 very obvious graben which strike NE across the associated volcanic plain (Pavri et al.,  
560 1992). Elsewhere, domes appear to converge on radial fracture patterns in surrounding  
561 terrains. Pavri et al. (1992) suggested that such relationships, and lineations in domes, dome  
562 clustering, evidence for interconnecting grabens and other surface lineations, are all  
563 evidence for shared feeder dykes. These features can also be explained by a fault-related  
564 extrusion model. Unfortunately, resolution in data means that it is challenging to accurately  
565 determine and infer relationships between domes and surrounding terrains. A fault controlled  
566 process of dome formation is, however, feasible.

567

568 Another significant difference between terrestrial and Venusian domes is surface conditions  
569 and the effects of weathering. Picrites near Marki were erupted onto a shallow Cretaceous  
570 seafloor, and at a pressure not dissimilar from that of the Venusian surface. However,  
571 temperature of the surface would have been significantly lower, and the palaeoseafloor  
572 preserved at Marki was first affected by seafloor processes, and has, since emergence,  
573 been shaped by active weathering processes. Bodies like Picrite Hill would originally have  
574 been concealed beneath sedimentary cover consisting of radiolarian mudstone, which is  
575 found adjacent to Picrite Hill (Fig.1), and deep-sea pelagic carbonates ranging from  
576 Maastrichtian to Oligocene in age (Lefkara formation) (Robertson 1997). Extensional faults in  
577 the Marki region, as well as facilitating eruption of crystal mush, also produced seafloor  
578 depressions which resulted in rapid accumulation of sediments, including, locally, thick  
579 umber deposits. However, background sediments are not found within Picrite Hill,  
580 suggesting that the body was erupted relatively soon after cessation of seafloor spreading  
581 and normal volcanism, and that extrusion, although pulsed, was rapid. Extensional faults are  
582 covered by sediments immediately to the north of Marki suggesting that they did not remain  
583 active for long after the end of magmatic activity. It is likely, therefore, that the  
584 palaeoseafloor at Marki was rapidly covered in sediment.

585

586 Field relationships demonstrate that although eruption of mush at Picrite Hill was facilitated  
587 by extensional faulting, this faulting had little influence on dome morphology. The extent to  
588 which the morphology of Picrite Hill has been modified by more recent weathering and  
589 erosion remains unclear. Although there is a clear difference in colour between UPL units  
590 and picrite, hardness and resistance to weathering appear to be similar. The Marki region is  
591 relatively arid and there are, currently, low rates of removal of material from the area  
592 adjacent to Picrite Hill, and low degrees of vegetation. Abrupt changes in dip between UPL  
593 and picrite units are consistent with formation of Picrite Hill as a steep-sided lava pile. The  
594 volume of material removed from this body is not clear. However, patterns in veining of UPL  
595 units immediately below and adjacent to Picrite Hill indicate that the lateral extent of the body  
596 was probably not significantly greater than presently outcropped. As such, the body appears  
597 to be well preserved, and clearly formed as a steep sided volcanic dome. Whilst the core of  
598 the body is more massive, thinner units on the sides and towards the top of Picrite Hill also  
599 suggest that crystal-rich lavas formed flows with relatively smooth, flat-tops. Spheroidal  
600 weathering gives parts of Picrite Hill a blocky appearance. However, examination of  
601 individual units suggests that erupted mush was closer in appearance to basaltic lava flows,  
602 rather than to rhyolitic flows.

603

604 The model for dome formation presented here should be readily testable in future, as it (1)  
605 implies that the domes are mafic to ultramafic rather than silica-rich, and (2) invokes an  
606 extensional-fault controlled mechanism for extrusion. The model implies that lavas forming  
607 volcanic domes are crystal-rich, and that non-hydrostatic stress provides a mechanism for  
608 mobilising crystal-rich mushes and facilitating eruption. The effects of crystal content, crystal  
609 size and crystal shape on magma viscosity remain poorly constrained. However, crystal-rich  
610 magmas are expected to be highly non-Newtonian, and the effect of increasing crystal  
611 content will be to increase viscosity by up to orders of magnitude (Champallier et al., 2008;  
612 Okumura et al., 2016). Pavri et al. (1992) used various modelling methods to constrain the  
613 effect of composition of dome morphology, and concluded that observed dome shapes and  
614 fracture patterns are consistent with silicic, high viscosity lava. However, as noted by Pavri et  
615 al. (1992), no single numerical approach produces a consistent model for dome formation,  
616 and the starting assumption for many models, i.e. Newtonian magma rheology, may be  
617 incorrect. Stofan et al. (2000) used an alternative approach to constrain dome composition,  
618 based on thermal models of crust development on erupted lava. They concluded that  
619 observed fracture patterns are consistent with fluid, lower viscosity interiors, at least for  
620 some of the domes observed in Magellan data. Petrographic examination and late-stage  
621 veining both demonstrate that erupted mush at Marki contained basaltic liquid. As such,  
622 extruded mush was a high temperature fluid, more comparable to basaltic lava. Superficially  
623 at least, such a mush would not be expected behave like a high viscosity rhyolitic liquid, and  
624 would not form a thick crust and blocky surface texture inconsistent with observed Venusian  
625 domes (Stofan et al., 2000). This is supported by observations at Marki. None of the units  
626 observed in the lava dome shows evidence for formation of thick crusts. Furthermore, in the  
627 adjacent area there are examples of pillowed picritic basalts. Although these have a lower  
628 olivine crystal content, their appearance does suggest that olivine-rich mushes behave more  
629 like high viscosity basalts than like rhyolites.

630  
631 Stofan et al. (2000) also suggested that surface depressions on some Venusian domes  
632 indicate a fluid dome interior. However, these features are not inconsistent with the proposed  
633 model of mush extrusion. As noted previously, parts of the core of Picrite Hill may have  
634 formed by injection of mush directly into the base of the lava pile. There is also a clear  
635 variation in lava viscosity between units, with limited flow of less crystal-rich units. It is,  
636 therefore, conceivable that ongoing eruption might produce lava domes on Venus with lower  
637 viscosity interiors. Importantly, there are considerable variations in dome morphology on  
638 Venus (e.g. Pavri et al. 1992), from flat-topped or shield-like domes, to domes with heavily  
639 fractured surfaces, domes with tiered shapes, complex shapes and domes with significant  
640 surface depressions. This complexity in morphology is not inconsistent with variations, both  
641 spatial and temporal, in magma viscosity as a function of crystal content, as observed at  
642 Marki.

643  
644 Finally, the model presented here does not require an additional magmatic process such as  
645 re-melting of parts of the Venusian crust. This is consistent with a simpler model for  
646 magmatism on Venus and similar stagnant-lid regime planets, where volcanism arises due  
647 to plume-related mantle melting, and where basaltic volcanism dominates. Uniquely, this  
648 model is able to account for marked differences in dome morphology compared to  
649 surrounding terrains, and also explains the intimate association of domes with basaltic lava  
650 plains. If correct, this crystal mush model may be applicable to other stagnant-lid bodies. The  
651 appearance of steep-sided domes on Venus might imply a unique, large-scale extensional  
652 mechanism which promotes extrusion of crystal mush. Alternatively, surface conditions on  
653 Venus might simply favour formation, preservation and ready identification of volcanic  
654 features formed by mush extrusion. This raises the possibility that mush extrusion occurred

655 on other bodies such as Mars, Mercury and the Moon during magmatically quiet periods,  
656 resulting in formation of distinct volcanic landforms.

657

658

659 **Acknowledgements:**

660 The authors would like to thank David A. Crown and Sami Mikhail, whose helpful comments  
661 and suggestions improved this manuscript considerably.

662 **References**

663

664 Anderson, S.W., Stofan, E.R., Plaut, J.J., and Crown, D.A., 1998, Block size distributions on  
665 silicic lava flow surfaces: Implications for emplacement conditions, *Geol. Soc. Am.*  
666 *Bull.*, 110, 1258-1267.

667 Airey, M.W., Mather, T.A., Pyle, D.M., Ghail, R.C., 2017. The distribution of volcanism in the  
668 Beta-Atla-Themis region of Venus: Its relationship to rifting and implications for global  
669 tectonic regimes. *J. Geophys. Res.* 122, 1626–1649.  
670 <https://doi.org/10.1002/2016JE005205>

671 Basilevsky, A.T., 1997. Venera 8 landing site geology revisited. *J. Geophys. Res.* 102,  
672 9257–9262. <https://doi.org/10.1029/97JE00413>

673 Bridges, N.T., 1997. Ambient effects on basalt and rhyolite lavas under Venusian, subaerial,  
674 and subaqueous conditions. *J. Geophys. Res.* 102, 9243–9255.  
675 <https://doi.org/10.1029/97JE00390>

676 Bridges, N.T., 1995. Submarine Analogs to Venusian Pancake Domes. *Geophys. Res. Lett.*  
677 22, 2781–2784. <https://doi.org/10.1029/95GL02662>

678 Champallier, R., Bystricky, M., Arbaret, L., 2008. Experimental investigation of magma  
679 rheology at 300 MPa: From pure hydrous melt to 76 vol.% of crystals. *Earth Planet. Sci.*  
680 *Lett.* 267, 571–583. <https://doi.org/10.1016/j.epsl.2007.11.065>

681 Constantinou, G., Govett, G.J.S., 1973. Geology, Geochemistry, and Genesis of Cyprus  
682 Sulfide Deposits. *Econ. Geol.* 68, 843–858. <https://doi.org/10.2113/gsecongeo.68.6.843>

683 Crumpler, L.S., Aubele, J.C., Senske, D.A., Keddie, S.T., Magee, K.P. and Head, J.W.,  
684 1993. Volcanoes and centers of volcanism on Venus. In *Venus II: Geology,*  
685 *Geophysics, Atmosphere and Solar Wind Environment*, eds Bougher S.W., Hunten  
686 D.M., Phillips, R.J. University of Arizona Press. ISBN 0-8165-1830-0.

687 Dilek, Y., Furnes, H., 2009. Structure and geochemistry of Tethyan ophiolites and their  
688 petrogenesis in subduction rollback systems. *Lithos* 113, 1–20.  
689 <https://doi.org/10.1016/j.lithos.2009.04.022>

690 Fink, J.H., Bridges, N.T., Grimm, R.E., 1993. Shapes of Venusian Pancake Domes Imply  
691 Episodic Emplacement and Silicic Composition. *Geophys. Res. Lett.* 20, 261–264.  
692 <https://doi.org/10.1029/92GL03010>

693 Ford, P.G., 1994. Radar Scattering Properties of Steep-sided Domes on Venus. *Icarus* 112,  
694 204–218. <https://doi.org/10.1006/icar.1994.1178>

695 Foster, A., Nimmo, F., 1996. Comparisons between the rift systems of East Africa, Earth and  
696 Beta Regio, Venus. *Earth Planet. Sci. Lett.* 143, 183–195. [https://doi.org/10.1016/0012-821X\(96\)00146-X](https://doi.org/10.1016/0012-821X(96)00146-X)

698 Gass, I.G., 1958. Ultrabasic Pillow Lavas from Cyprus. *Geol. Mag.* 95, 241–251.

699 Gass, I.G., 1968. Is Troodos Massif of Cyprus a Fragment of Mesozoic Ocean Floor. *Nature*  
700 220, 39-. <https://doi.org/10.1038/220039a0>

701 Gregg, T.K.P., Fink, J.H., 1996. Quantification of extraterrestrial lava flow effusion rates  
702 through laboratory simulations. *J. Geophys. Res.* 101, 16891–16900.  
703 <https://doi.org/10.1029/96JE01254>

704 Guest, J.E., Bulmer, M.H., Aubele, J., Beratan, K., Greeley, R., Head, J.W., Michaels, G.,  
705 Weitz, C., Wiles, C., 1992. Small volcanic edifices and volcanism in the plains of Venus.  
706 *J. Geophys. Res.* 97, 15949–15966. <https://doi.org/10.1029/92JE01438>

707 Hansen, V. L. (2005). Venus's shield terrain. *Bulletin of the Geological Society of America*,  
708 117(5-6), 808-822. <https://doi.org/10.1130/B256060.1>

709 Ivanov, M.A., 2015. Volcanic complexes on Venus: Distribution, age, mechanisms of origin,  
710 and evolution. *Petrology* 23, 127–149. <https://doi.org/10.1134/S0869591115020046>

711 Ivanov, M.A., Head, J.W., 2015. The history of tectonism on Venus: A stratigraphic analysis.  
712 *Planet. Space Sci.* 113, 10–32. <https://doi.org/10.1016/j.pss.2015.03.016>

713 Ivanov, M.A., Head, J.W., 2011. Global geological map of Venus. *Planet. Space Sci.* 59,  
714 1559–1600. <https://doi.org/10.1016/j.pss.2011.07.008>

715 Ivanov, M.A., Head, J.W., 1999. Stratigraphic and geographic distribution of steep-sided  
716 domes on Venus: Preliminary results from regional geological mapping and implications

717 for their origin. *J. Geophys. Res.* 104, 18907–18924.  
718 <https://doi.org/10.1029/1999JE001039>

719 Karato, S., Barbot, S., 2018. Dynamics of fault motion and the origin of contrasting tectonic  
720 style between Earth and Venus. *Sci. Rep.* 8. [https://doi.org/10.1038/s41598-018-30174-](https://doi.org/10.1038/s41598-018-30174-6)  
721 6

722 Kaula, W.M., 1990. Venus - A Contrast in Evolution to Earth. *Science* (80). 247, 1191–1196.  
723 <https://doi.org/10.1126/science.247.4947.1191>

724 Malpas, J., Langdon, G., 1984. Petrology of the Upper Pillow Lava suite, Troodos ophiolite,  
725 Cyprus, in: Gass, I.G., Lippard, S.J., Shelton, A.W. (Eds.), *Ophiolites and Oceanic*  
726 *Lithosphere*. Geological Society, London, Special Publication No. 13, pp. 155–167.

727 Marsh, B.D., 1981. On the Crystallinity, Probability of Occurrence, and Rheology of Lava  
728 and Magma. *Contrib. Mineral. Petrol.* 78, 85–98. <https://doi.org/10.1007/BF00371146>

729 McKenzie, D., Ford, P.G., Liu, F., Pettengill, G.H., 1992. Pancake-like Domes on Venus. *J.*  
730 *Geophys. Res.* 97, 15967–15976. <https://doi.org/10.1029/92JE01349>

731 Mikhail, S., Heap, M.J., 2017. Hot climate inhibits volcanism on Venus: Constraints from rock  
732 deformation experiments and argon isotope geochemistry. *Phys. Earth Planet. Inter.*  
733 268, 18–34. <https://doi.org/10.1016/j.pepi.2017.05.007>

734 Mukasa, S.B., Ludden, J.N., 1987. Uranium-lead isotopic ages of plagiogranites from the  
735 troodos ophiolite, cyprus, and their tectonic significance. *Geology* 15, 825–828.  
736 [https://doi.org/10.1130/0091-7613\(1987\)15<825:UUAOPF>2.0.CO;2](https://doi.org/10.1130/0091-7613(1987)15<825:UUAOPF>2.0.CO;2)

737 Okumura, S., Kushnir, A.R.L., Martel, C., Champallier, R., Thibault, Q., Takeuchi, S., 2016.  
738 Rheology of crystal-bearing natural magmas: Torsional deformation experiments at 800  
739 degrees C and 100 MPa. *J. Volcanol. Geotherm. Res.* 328, 237–246.  
740 <https://doi.org/10.1016/j.jvolgeores.2016.11.009>

741 Pavri, B., Head, J.W., Klose, K.B., Wilson, L., 1992. Steep-sided domes on venus -  
742 characteristics, geologic setting, and eruption conditions from magellan data. *J.*  
743 *Geophys. Res.* 97, 13445–13478. <https://doi.org/10.1029/92JE01162>

744 Pearce, J.A., Robinson, P.T., 2010. The Troodos ophiolitic complex probably formed in a  
745 subduction initiation, slab edge setting. *Gondwana Res.* 18, 60–81.  
746 <https://doi.org/10.1016/j.gr.2009.12.003>

747 Plaut, J.J., Anderson, S.W., Crown, D.A., Stofan, E.R., van Zyl, J.J., 2004. The unique radar  
748 properties of silicic lava domes. The unique radar properties of silicic lava domes. *J.*  
749 *Geophys. Res.* 109. <https://doi.org/10.1029/2002JE002017>

750 Quick, L.C., Glaze, L.S., Baloga, S.M., Stofan, E.R., 2016. New approaches to inferences for  
751 steep-sided domes on Venus. *J. Volcanol. Geotherm. Res.* 319, 93–105.  
752 <https://doi.org/10.1016/j.jvolgeores.2016.02.028>

753 Robertson, A.H., Hudson, J.D., 1973. Cyprus umbers - chemical precipitates on a tethyan  
754 ocean ridge. *earth Planet. Sci. Lett.* 18, 93–101. [https://doi.org/10.1016/0012-](https://doi.org/10.1016/0012-821X(73)90039-3)  
755 821X(73)90039-3

756 Robertson, A., 2004. Development of concepts concerning the genesis and emplacement of  
757 Tethyan ophiolites in the Eastern Mediterranean and Oman regions. *Earth-Science*  
758 *Rev.* 66, 331–387. <https://doi.org/10.1016/j.earscirev.2004.01.005>

759 Robertson, A.H.F., Xenophontos, C., 1997. Cyprus, in: *Encyclopedia of European and Asian*  
760 *Regional Geology*. Springer Netherlands, Dordrecht, pp. 160–171.  
761 [https://doi.org/10.1007/1-4020-4495-X\\_23](https://doi.org/10.1007/1-4020-4495-X_23)

762 Sakimoto, S.E.H., Zuber, M.T., 1995. The spreading of variable-viscosity axisymmetrical  
763 radial gravity currents - applications to the emplacement of venusian pancake domes.  
764 *J. Fluid Mech.* 301, 65–77. <https://doi.org/10.1017/S0022112095003806>

765 Saunders, R.S., Arvidson, R.E., Head, J.W., Schaber, G.G., Stofan, E.R., Solomon, S.C.,  
766 1991. An overview of Venus geology. *Science* 252, 249–252.  
767 <https://doi.org/10.1126/science.252.5003.249>

768 Searle, D.L., Vokes, F.M., 1969. Layered ultrabasic lavas from cyprus. *Geol. Mag.* 106, 515-  
769 <https://doi.org/10.1017/S001675680005929X>

770 Shellnutt, J.G., 2018. Derivation of intermediate to silicic magma from the basalt analyzed at  
771 the Vega 2 landing site, Venus. *PLoS One* 13.

772 <https://doi.org/10.1371/journal.pone.0194155>  
773 Shellnutt, J.G., 2013. Petrological modeling of basaltic rocks from Venus: A case for the  
774 presence of silicic rocks. *J. Geophys. Res.* 118, 1350–1364.  
775 <https://doi.org/10.1002/jgre.20094>  
776 Smith, D.K., 1996. Comparison of the shapes and sizes of seafloor volcanoes on Earth and  
777 “pancake” domes on Venus. *J. Volcanol. Geotherm. Res.* 73, 47–64.  
778 [https://doi.org/10.1016/0377-0273\(96\)00007-8](https://doi.org/10.1016/0377-0273(96)00007-8)  
779 Solomatov, V.S., Moresi, L.N., 1996. Stagnant lid convection on Venus. *J. Geophys. Res.*  
780 101, 4737–4753. <https://doi.org/10.1029/95JE03361>  
781 Stofan, E.R., Anderson, S.W., Crown, D.A., Plaut, J.J., 2000. Emplacement and composition  
782 of steep-sided domes on Venus. *J. Geophys. Res.* 105, 26757–26771.  
783 <https://doi.org/10.1029/1999JE001206>  
784 Tanaka, K.L., Senske, D.A., Price, M., Kirk, R.L., 1997. Physiography,  
785 geomorphic/geological mapping, and stratigraphy of Venus. In *Venus II: Geology,*  
786 *Geophysics, Atmosphere and Solar Wind Environment*, eds Bougher S.W., Hunten  
787 D.M., Phillips, R.J. University of Arizona Press. ISBN 0-8165-1830-0.  
788 Woelki, D., Regelous, M., Haase, K.M., Romer, R.H.W., Beier, C., 2018. Petrogenesis of  
789 boninitic lavas from the Troodos Ophiolite, and comparison with Izu-Bonin-Mariana  
790 fore-arc crust. *Earth Planet. Sci. Lett.* 498, 203–214.  
791 <https://doi.org/10.1016/j.epsl.2018.06.041>  
792

